PCCP

Accepted Manuscript

This is an *Accepted Manuscript*, which has been through the Royal Society of Chemistry peer review process and has been accepted for publication.

Accepted Manuscripts are published online shortly after acceptance, before technical editing, formatting and proof reading. Using this free service, authors can make their results available to the community, in citable form, before we publish the edited article. We will replace this *Accepted Manuscript* with the edited and formatted *Advance Article* as soon as it is available.

You can find more information about *Accepted Manuscripts* in the Information for Authors.

Please note that technical editing may introduce minor changes to the text and/or graphics, which may alter content. The journal's standard Terms & Conditions and the Ethical guidelines still apply. In no event shall the Royal Society of Chemistry be held responsible for any errors or omissions in this *Accepted Manuscript* or any consequences arising from the use of any information it contains.

ROYAL SOCIETY OF CHEMISTRY

www.rsc.org/pccp

Cite this: DOI: 10.1039/c0xx00000x

www.rsc.org/xxxxxx

ARTICLE TYPE

One-step fabrication of ultralong nanobelts of PI-PTCDI and its optoelectronic properties

Bo Yang [a,b], Feng-Xia Wang[a], Kai-Kai Wang[a], Jing-Hui Yan[*b], Yong-Qiang Liu[a], and Ge-Bo Pan[*a]

Received (in XXX, XXX) Xth XXXXXXXXX 20XX, Accepted Xth XXXXXXXXX 20XX

DOI: 10.1039/b000000x

The ultralong nanobelts of N,N-bis-(1-propylimidazole)-3,4,9,10-perylene tetracarboxylic diimide (PI-PTCDI) were fabricated by one-step solution process. The prototype devices based on the PI-PTCDI nanobelts exhibited excellent photodetector and photoswitching performance. The highest I_{on}/I_{off} ratio and photoresponsivity of photodiode could reach 240 and 5.6 mA/W, respectively.

Organic photodetectors (OPDs) have attracted increasing interest due to their high sensitivity, low noise, conformal flexibility, and good adaptability.[1] In general, both n-type and p-type organic semiconductors (OSs) can be used as the active layers of OPDs. The photodetector performance of n-type OSs is outmatched by that of burgeoning p-type counterparts due to their low electron mobility and stability.[2-5] It is still a great challenge to develop n-type OSs with high mobility and good ambient stability. Perylene tetracarboxylic diimide (PTCDI) and its derivatives are one of the most important types of n-type OSs with high thermal stability, photo stability, and carrier mobility.[6-12]

To date, numerous PTCDI molecules have been synthesized by inserting different side chains onto the imide position of pristine PTCDI.[7-10] It is confirmed that the side chains play a vital role in controlling the molecular packing, morphology, and subsequently optoelectronic properties of PTCDI assemblies.[9,13] However, it is noted that most of side chains are long alkyls in previous studies. There are very limited studies on the synthesis and self-assembly of PTCDI molecules with heterocyclic units (such as imidazole and pyridine),[14] although they are of particular interest in forming hydrogen bonds, thus affecting their self-assembling behaviour and optoelectronic properties.

Here, we report the synthesis and self-assembly of N,N-bis-(1-propylimidazole)-3,4,9,10-perylene tetracarboxylic diimide (PI-PTCDI, Scheme 1). The targeted PI-PTCDI molecule can easily self-assemble into ultralong nanobelts by a facile solution process. The prototype photodetectors based on nanobelt network exhibit excellent reproducibility and stability. The nanobelts show highly photosensitive and photoresponsive characteristics. To the best of our knowledge, such high-performance photodetectors based on one-dimensional (1D) nanostructures of PTCDI molecules with heterocyclic units are almost unexplored.

The procedure for the synthesis of PI-PTCDI was similar to the literature (Scheme 1, Fig. S1 and S2, †ESI).[14] In a typical synthesis, the PI-PTCDI powder was dissolved into chloroform with sonication at 50 °C for 1 h. The solution was filtered by using 0.22 μm filter head and injected in methanol (V_{CHCl3}/V_{CH3OH} = 1:40). The mixed solution was stored at room temperature for about 2 days. The final solution was transparent and the precipitates were collected at the bottom.

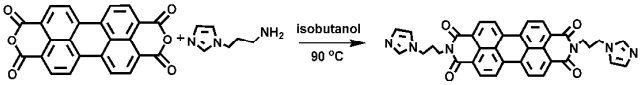

Scheme 1. Chemical structure and synthesis route of PI-PTCDI.

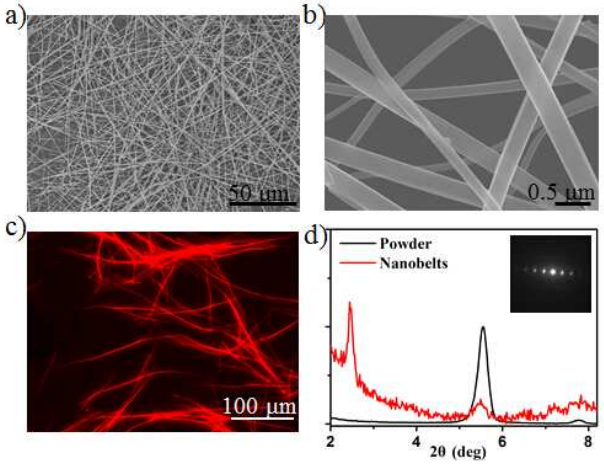

Fig. 1 (a) and (b) Typical SEM images of PI-PTCDI nanobelts. (c) Fluorescence optical microscopy image of PI-PTCDI nanobelts. (d) XRD spectra of nanobelts and source powder of PI-PTCDI. The inset is an SAED pattern recorded with a single PI-PTCDI nanobelt. The volume ratio of V_{CHCl3}: V_{CH3OH} was 1:40.

Fig. 1a and 1b present typical scanning electron microscopy (SEM) images of the product. The volume ratio of chloroform to methanol (V_{CHCl3}/V_{CH3OH}) is 1:40. The images indicate that the nanobelt structures with smooth surfaces are formed. The average width of nanobelts is ~ 200 nm and the length is up to ~300 μm. It is noted that the width and length don't change significantly with the volume ratio of V_{CHCl3}/V_{CH3OH}. In present study, the PI-PTCDI is made from perylene and imidazole (Scheme 1). That is, the strong π-π interaction between the perylene planes and the H-bond interaction between the imidazole should be taken into account for the self-assembly of PI-PTCDI. Moreover, the as-prepared nanobelts could emit strong fluorescence as depicted in the fluorescence microscopy image (Fig. 1c). The strong red

Physical Chemistry Chemical Physics Accepted Manuscript

fluorescence of the nanobelts can be easily observed even with naked eyes, making the nanobelts more feasible to be used in fluorescence sensing. Fig. 1d show the X-ray diffraction (XRD) patterns of both nanobelts and source powder of PI-PTCDI. In comparison with that of source powder, an additional diffraction peak is observed around 2.5 °. This is possibly attributed to the preferential growth of high-aspect-ratio nanobelts, which are driven by strong molecular stacking between PI-PTCDI skeletons. Moreover, this sharp peak also indicates that the nanobelts have a highly crystalline feature. This is further confirmed with the well-defined selected-area electron diffraction (SAED) pattern of a single nanobelt, as shown in the inset of Fig. 1d.

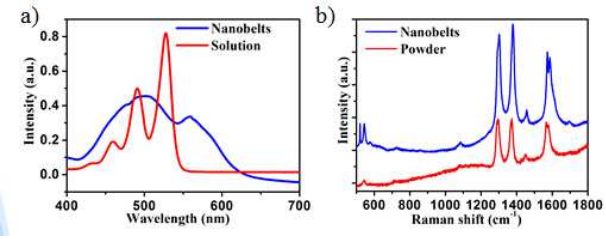

Fig. 2 (a) UV-vis absorption and (b) Raman spectra of nanobelts and source powder of PI-PTCDI.

The chemical composition of nanobelts is analyzed by the Fourier transform infrared spectroscopy (FT-IR) and the energy dispersive X-ray diffraction spectroscopy (EDX). It is found that the FT-IR spectrum of nanobelts has the same feature as that of source powder of PI-PTCDI (Fig. S3a, †ESI). The characteristic bands of carbonyl groups of -CO-NH-CO-, benzene ring skeleton vibrations, methylene vibration, C=C vibration of imidazole ring are observed.[15] This indicates that PI-PTCDI molecules do not undergo decomposition or other chemical reactions during the self-assembling process. However, the benzene ring stretch, and C-H bend peaks in the FT-IR of nanobelts are slightly shifted to higher wave numbers. This implies that stronger π-π interaction is formed between PI-PTCDI molecules in the nanobelts than those in source powder.[16] In addition, the EDX spectrum (Fig. S3b, †ESI) only shows the peaks of C, N and O elements, indicating that $CHCl_3$ is not involved in the PI-PTCDI nanobelts.

To explore the optical properties of PI-PTCDI nanobelts, both UV-vis absorption and Raman spectra are recorded. Fig. 2a shows the absorption spectra of PI-PTCDI dissolved in $CHCl_3$ solution and the nanobelts deposited on quartz. The spectrum of PI-PTCDI solution shows three pronounced peaks in the range of 450-525 nm and a small shoulder around 425 nm. This is a typical spectrum of individual PI-PTCDI molecules in solution (i.e., in a non-aggregated form), corresponding to an electronic π-π* transition superimposed with vibrational transitions.[17] In contrast, the spectrum of nanobelts shows dramatic changes with a wide absorption band in visible region, together with a peak at around 558 nm. These peaks of nanobelts correspond to the S_0-S_1 electronic superimposed with vibrational transitions. Moreover, the emission from nanobelts centres at 670 nm, which is red-shifted by ~ 50 nm relative to that of source powder (Fig. S4, †ESI). The above spectra changes indicate strong molecular stacking between the PI-PTCDI skeletons. Moreover, the pronounced absorption band emerging at longer wavelength is typically a sign of the effective π-π interaction in co-facial configuration of molecular stacking.[10] These results indicate that strong π-π* stacking interaction of perylene chromophores is the main driving force for the formation of nanobelts.[17] Moreover, the Raman spectrum (Fig. 2b) of nanobelts has the same features as that of source powder of PI-PTCDI. Four strong characteristic peaks of 540, 1294, 1373 and 1572 cm^{-1} are observed and agree well with the literature.[15] In addition, it is noted that the Raman peaks of nanobelts has a little red shift compared with the powder, which might be ascribed to a stronger π-π accumulation effect between PI-PTCDI molecules.

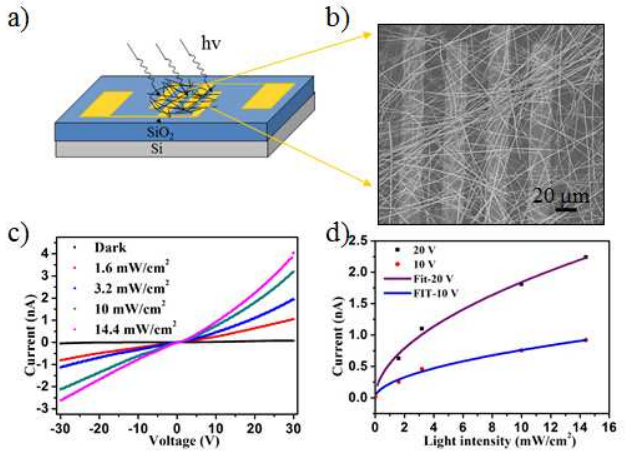

Fig. 3 (a) Schematic illustration and (b) SEM image of device based on a network film of PI-PTCDI nanobelts. (c) Dark current and photocurrents at different incident power densities. (d) Photocurrents versus incident optical densities measured at bias voltages of 10 V and 20 V.

The photoresponse characteristics have been investigated by fabricating the prototype photoelectric device of network films of PI-PTCDI nanobelts. Fig. 3a and 3b show a schematic illustration and an SEM image of the device, respectively. The morphology and fabrication process of the finger electrodes are the same as the reported device.[18] The nanobelts are fabricated at 1:40 of the volume ratio of V_{CHCl3}/V_{CH3OH}, which are similar to those shown in Fig. 1a. The methanol solution dispersed the nanobelts is dropped on the surface of Au electrodes. It is clear that the nanobelt network has been connected to two Au electrodes. Fig. 3c shows the typical *I-V* curves of the device in the dark and under continuous white light illumination with varying intensity. The device based on PI-PTCDI nanobelts film exhibits excellent photoresponse characteristics. The photocurrent under light illumination is markedly higher than that obtained in the dark. At the bias of 10 V, the nanobelts network in dark exhibits a relatively low current of 3.47 pA. Simultaneously a high current of about 239 pA is obtained even under a low power irradiation of 1.6 mW/cm^2. This corresponded to a photocurrent ratio of about 68. As expected, with the increase of the power density, the photocurrent on/off ratio can be raised, which can be attributed to the change in photo-generated carriers at different incident light densities.[19] At a high power density of 14.4 mW/cm^2, the photocurrent on/off ratio can reach 222. Moreover, the photocurrent can increase with the light intensity (Fig. 3c). Fig. 3(d) shows the relationship between the photocurrent and incident

Physical Chemistry Chemical Physics Accepted Manuscript

This journal is © The Royal Society of Chemistry [year]

light power densities. This can be well fitted with a simple power law,[19] $Ip \sim P^{\theta}$, where θ determines the response of the photocurrent to light intensity. The fitting demonstrates a power dependence of ~ 0.53 at 20 V, and 0.52 at 10 V, which is $I \sim P^{0.53}$ or $I \sim P^{0.52}$. The non-unity ($0.5 < \theta < 1$) exponent suggests a complex process of electron-hole generation, recombination, and trapping within a semiconductor.[20] The characteristic indicates an excellent photo-capture in the PI-PTCDI nanobelts film.

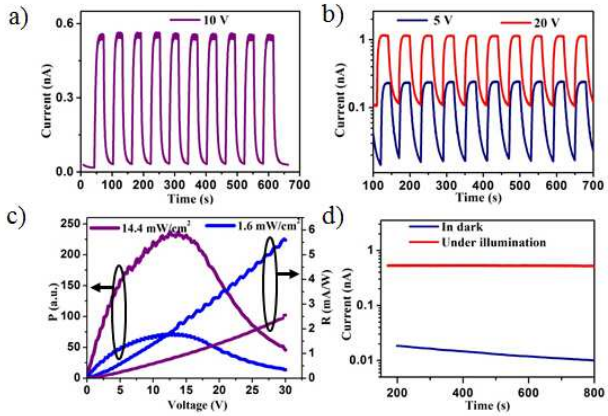

Fig. 4 (a) and (b) Time-dependent on/off switching of device based on PI-PTCDI nanobelts. (c) Photoresponsivity (R) and photocurrent/dark current ratio (P) versus Vbias under illumination with 1.6 mW/cm^2 and 14.4 mW/cm^2. (d) Current versus time continuously over 800 s in dark and under illumination.

Moreover, the time-dependent photoresponse of devices has been demonstrated to be prompt and reversible by turning on and off the white light. Fig. 4a shows the typical on/off characteristics with the light turning on and off. The light power is 14.4 mW/cm^2 and the applied voltage is 10 V. It is clear that the current of devices shows two distinct states, a "low" current state in the dark and a "high" current state under white light illumination. The "on"- and "off"-state currents for 10 cycles remain almost the same and the switching in the two states is very fast and reversible (Fig. 4a, 4b), implying not only fast photosensitive but also the high stability of the materials. The above excellent performance proves the promising potential application of PI-PTCDI nanobelts in the low-cost, high-performance photo switching and photodetector devices.

The photosensitivity (I_{light}/I_{dark} ratio, P) and photoresponsivity (R) are two important parameters for photodetector.[3] As shown in Fig. 4c, the P varies with the applied voltage and light intensity. The P_{max} can reach 240. In addition, it is seen that the R is also dependent on the voltage except the light intensity, which rises with increasing of applied voltage, indicating some field-assisted exciton dissociation close to the interface.[19] The calculated maximum of R reaches to 5.6 mA/W at 30 V under illumination intensity of 1.6 mW/cm^2. The value can be competed that the reported literature.[21] Importantly, the device shows high the photo-current durability and environmental stability. As shown in Fig. 4d, the current in dark starts to degrade relatively slowly and finally remains almost constant, while the photocurrent at 10 V with illumination intensity of 14.4 mW/cm^2 nearly holds steady. After 800 s, the photocurrent only decreases by 2.0 %. A similar phenomenon has been reported in the literature and is possibly attributed to the traps and other defect states in the semiconductor nanomaterials.[22]

In summary, PI-PTCDI with imidazole units was synthesized and self-assembled into nanobelts, which were uniform, ultralong, and highly crystalline. The as-prepared nanobelts were directly employed for the construction of prototype photodetectors. The devices exhibited excellent photodetector performances with high reproducibility and stability. The photocurrent only decreased by 2.0 % after 800 s. Moreover, the ultralong nanobelts exhibited highly photosensitive and photoresponsive characteristics, which had an I_{light}/I_{dark} ratio of 240 and a photoresponsivity of 5.6 mA/W. The results suggested the potential application of PTCDI nanobelt devices for high-sensitivity and high-stability nanoscale photodetectors and photoelectrical switches.

Acknowledgement

This work was financially supported by the National Natural Science Foundation of China (Nos. 21273272 and 21303250), the Jiangsu Province Natural Science Foundation of China (No. BK2012192), the National Basic Research Program of China (No. 2010CB934100), and the Chinese Academy of Sciences.

Notes and references

[a] *Suzhou Institute of Nano-tech and Nano-bionics, Chinese Academy of Sciences, 215123 Suzhou, P. R. China, Fax: +86-512-62872663.*
E-mail address: gbpan2008@sinano.ac.cn
[b] *College of Chemistry and Environmental Engineering, Changchun University of Science and Technology, 130022 Changchun, China.*
E-mail address: yjh@cust.edu.cn

† Electronic Supplementary Information (ESI) available: [Experimental details, ^{1}HNMR, ^{13}CNMR, HRMS, EDX, FT-IR, and emission spectra of PI-PTCDI nanobelts]. See DOI: 10.1039/b000000x/

1 H. Dong, H. Zhu, Q. Meng, X. Gong and W. Hu, *Chem. Soc. Rev.*, 2012, **41**, 1754.
2 Y. K. Che, X. M. Yang, G. L. Liu, C. Yu, H. W. Ji, J. M. Zuo, J. C. Zhao and L. Zang, *J. Am. Chem. Soc.*, 2010, **132**, 5743-5750.
3 H. Yu, Z. Bao and J. H. Oh, *Adv. Funct. Mater.* 2013, **23**, 629-639.
4 W-Y. Chou, Y.-S. Lin, L.-L.Kuo, S.-J. Liu, H.-L. Cheng and F.-C. Tang, *J. Mater. Chem. C*, 2014, **2**, 626-632.
5 B. Narayan, S. P. Senanayak, A. Jain, K. S. Narayan, and S. J. George, *Adv. Funct. Mater.* 2013, **23**, 3053.
6 A. L. Briseno, S. C. B. Mannsfeld, C. Reese, J. M. Hancock, Y. J. Xiong, S. A. Jenekhe, Z. N. Bao, and Y. N. Xia, *Nano. Lett.*, 2007, **7**, 2847-2853.
7 L. Zang, Y. Che and J. S. Moore, *Acc. Chem. Res.*, 2008, **41**, 1596-1608.
8 A. Datar and K. Balakrishnan and L. Zang, *Chem. Commun.*, 2013, **49**, 6894-6896.
9 Y. K. Che, X. M. Yang, K. Balakrishnan, J. M. Zuo and L. Zang, *Chem. Mater.*, 2009, **21**, 2930-2934.
10 K. Balakrishnan, A. Datar, T. Naddo, J. L. Huang, R. Oitker, M. Yen, J. C. Zhao, and L. Zang, *J. Am. Chem. Soc.*, 2006, **128**, 7390-7398.
11 C. Grimsdale and K. Müllen, *Angew. Chem., Int. Ed.*, 2005, **44**, 5592-5629.
12 Y. Che, A. Datar, K. Balakrishnan, and L. Zang, *J. Am. Chem. Soc.* 2007, **129**, 7234.
13 F. Würthner, *Chem. Commun*, 2004, 1564.
14 Y. Hu, K. Wang, Q. Zhang, F. Li, T. Wu and L. Niu, *Biomaterials*, 2012, **33**, 1097-1106.
15 V. Chiş, G. Mile, R. Ştiufiuc, N. Leopold and M. Oltean, *J. Mol. Struct.*, 2009, **924-926**, 47-53.
16 H. F. Ji, R. Majithia, X. Yang, X. H. Xu, and K. More, *J. Am. Chem. Soc.*, 2008, **130**, 10056-10057.

Physical Chemistry Chemical Physics Accepted Manuscript

17 Y. W. Huang, B. G. Quan, Z. X. Wei, G. T. Liu and L. F. Sun, *J. Phys. Chem. C*, 2009, **113**, 3929-3933.
18 F.-X. Wang, Y.-Q. Liu, H.-D. Wu, Y. Xiao and G.-B. Pan, *J. Mater. Chem. C*, 2013, **1**, 422-425.
19 X. Zhang, J. Jie, W. Zhang, C. Zhang, L. Luo, Z. He, X. Zhang, W. Zhang, C. Lee, and S. Lee, *Adv. Mater*. 2008. **20**, 2427.
20 L. Li, P. S. Lee, C. Y. Yan, T. Y. Zhai, X. S. Fang, M. Y. Liao, Y. Koide, Y. Bando, and D. Golberg, *Adv. Mater.*, 2010, **22**, 5145-5149.
21 B. Mukherjee, M. Mukherjee, K. Sim and S. Pyo, *J. Mater. Chem.*, 2011, **21**, 1931-1936.
22 Y. Jiang, W. J. Zhang, J. S. Jie, X. M. Meng, X. Fan and S. T. Lee, *Adv. Funct. Mater.*, 2007, **17**, 1795-1800.

Physical Chemistry Chemical Physics Accepted Manuscript

This journal is © The Royal Society of Chemistry [year]